Clim. Past Discuss., 9, 2115–2152, 2013
www.clim-past-discuss.net/9/2115/2013/
doi:10.5194/cpd-9-2115-2013

Climate of the Past Discussions
Open Access

The role of East-Tethys seaway closure in the middle Miocene climatic transition (ca. 14 Ma)

N. Hamon[1,2], P. Sepulchre[2], V. Lefebvre[3,2], and G. Ramstein[2]

[1]Institut de Paléoprimatologie, Paléontologie Humaine: Evolution et Paléoenvironnements, CNRS-INEE-Université de Poitiers, Poitiers, France
[2]Laboratoire des Sciences du Climat et de l'Environnement, UMR8212, CEA-CNRS-Université de Versailles Saint-Quentin-en-Yvelines, Gif-sur-Yvette, France
[3]Géosciences Environnement Toulouse, CNRS-UPS-IRD-CNES, Toulouse, France

Received: 15 March 2013 – Accepted: 28 March 2013 – Published: 15 April 2013

Correspondence to: N. Hamon (noemie.hamon@lsce.ipsl.fr)

Published by Copernicus Publications on behalf of the European Geosciences Union.

Abstract

The middle Miocene climatic transition (MMCT, approximately 14 Ma) is a key period in Cenozoic cooling and cryospheric expansion. Despite it is well documented in isotopic record, the causes of the MMCT are still a matter of debate. Among various hypotheses, some authors suggested that it was linked with the final closure of the East-Tethys seaway and subsequent oceanic circulation reorganisation. The aim of the present study is to quantify the impact of varying East-Tethys seaway depths on middle Miocene ocean and climate, in order to better understand its role in the MMCT.

We present four sensitivity experiments with a fully coupled ocean-atmosphere generalized circulation model. Our results indicate the presence of a warm and salty water source in the northern Indian Ocean when the East-Tethys is deep-open (4000 or 1000 m), which corresponds to the Tethyan Indian Saline Water (TISW) described on the basis of isotopic studies. This water source is absent in the experiments with shallow (250 m) and closed East-Tethys, inducing strong changes in the latitudinal density gradient and ultimately the reinforcement of the Antarctic Circumpolar Current (ACC). Moreover, when the East-Tethys seaway is shallow or closed, there is a westward water flow in the Gibraltar Strait that strengthens the Atlantic meridional overturning circulation (AMOC) compared to the experiments with deep-open East-Tethys. Our results therefore suggest that the shoaling and final closure of the East-Tethys seaway played a major role in the oceanic circulation reorganisation during the middle Miocene.

The results presented here provide new constraints on the timing of the East-Tethys seaway closure, and particularly indicate that, prior to 14 Ma, a deep-open East-Tethys should have allow the formation of TISW. Moreover, whereas the final closure of this seaway likely played a major role in the MMCT, we suggest that it was not the only driver of the global cooling and Antarctica ice sheet growth. Here, we propose that the initiation of the MMCT may have been an atmospheric pCO_2 drawdown and that the oceanic Changes due to the East-Tethys seaway closure amplified the response of global climate and East-Antarctic Ice Sheet.

CPD
9, 2115–2152, 2013

1 Introduction

Isotopic studies indicate that the middle Miocene epoch was crucial regarding the Cenozoic global cooling and Antarctic ice-sheet expansion (Zachos et al., 2001; Billups and Schrag, 2002; Shevenell et al., 2004). In particular, the middle Miocene climatic transition (MMCT), approximately 14.2 to 13.8 Ma, was a period of rapid global cooling and Antarctic Ice Sheet growth (Zachos et al., 2001; Billups and Schrag, 2002; Shevenell et al., 2004). This transition is marked, in marine carbonates $\delta^{18}O$, by a two-step increase of approximately 1 ‰, which is interpreted as the consequence of a global cooling of approximately 3 °C in the deep ocean (Billups and Schrag, 2002), as well as the development of the East-Antarctic Ice Sheet (Woodruff and Savin, 1989; Flower and Kennett, 1994; Zachos et al., 2001; Billups and Schrag, 2002; Shevenell et al., 2004). A major reorganisation of oceanic circulation was also inferred from oceanic data. The Antarctic Circum-polar Current (ACC) was notably reinforced, and the southern frontal system moved northward during the middle Miocene (Shevenell et al., 2004; Kuhnert et al., 2009; Verducci et al., 2009).

Although it is well documented in both continental and oceanic data, the causes of the MMCT are still highly debated (Zachos et al., 2001; Billups and Schrag, 2002; Shevenell et al., 2004, 2008; Mosbrugger et al., 2005; Bruch et al., 2007; Utescher et al., 2011). Some authors argue that it was due to an atmospheric CO_2 concentration drawdown (Shevenell et al., 2004; Holbourn et al., 2005; Tripati et al., 2009), but pCO_2 variations during the Miocene are not well constrained (Cerling, 1991; Pagani et al., 1999, 2009; Pearson and Palmer, 2000; Royer et al., 2001; Kürschner et al., 2008; Kürschner and Kvacek, 2009; Tripati et al., 2009). Indeed the reconstructions for the middle Miocene climatic optimum (approximately 17–15 Ma) are controversial, varying from 200 to 700 ppmv, whereas the majority of published studies agree that the atmospheric pCO_2 was low (approximately 200–300 ppmv) during the MMCT (Cerling, 1991; Pagani et al., 1999, 2009; Pearson and Palmer, 2000; Royer et al., 2001; Kürschner et al., 2008; Kürschner and Kvacek, 2009; Tripati et al., 2009). Another

CPD
9, 2115–2152, 2013

view is that insolation should have played an important role in the East-Antarctic Ice Sheet growth (Shevenell et al., 2004, 2008; Holbourn et al., 2005), and modeling studies suggested that, at low atmospheric CO_2 concentration, orbital configuration is a major driver of ice-sheet development (Deconto et al., 2007).

Geographic changes have also been invoked to explain the middle Miocene climatic transition. In particular, some authors suggested that it was initiated by the final closure of the East-Tethys seaway, and the end of water exchanges between the Indian Ocean and the Paratethys (Woodruff and Savin, 1989; Wright et al., 1992; Flower and Kennett, 1994; Flower and Kennett, 1995). Although the timing of the East-Tethys seaway closure is still under debate, isotopic and biological proxies indicate that the Paratethys and the Indian Ocean were connected until approximately 14 Ma (Rögl, 1999; Harzhauser and Piller, 2007; Harzhauser et al., 2009; Okay et al., 2010; de Leeuw et al., 2013). Moreover, carbon and oxygen isotopic composition in benthic and planctonic foraminifera suggest that, prior to 14 Ma, a warm and saline water mass (the so-called Tethyan Indian Saline Water, hereafter TISW) transported heat from the East Tethys to the southern Indian Ocean (Woodruff and Savin, 1989; Wright et al., 1992; Flower and Kennett, 1994; Flower and Kennett, 1995). The presence of this warm water in the Southern Ocean should have been associated with a slow ACC, preventing the East-Antarctic Ice Sheet growth (Woodruff and Savin, 1989; Wright et al., 1992). Around 14 Ma, the final closure of the East-Tethys seaway would have terminated the formation of the TISW. Ultimately, this should have allowed ice sheet growth through three hypothesized mechanisms: (i) decrease in southward heat transport (Woodruff and Savin, 1989; Flower and Kennett, 1994; Flower and Kennett, 1995), (ii) acceleration of the ACC (Flower and Kennett, 1995; Kuhnert et al., 2009; Verducci et al., 2009) and (iii) enhancement of North Atlantic Deep Water production and meridional heat transport, driving an increase in evaporation over the Southern Ocean and ultimately more precipitation over Antarctica (Wright et al., 1992).

In the present study, we investigate the impact of the East-Tethys seaway closure on middle Miocene oceanic circulation and climate. We perform sensitivity experiments

CPD
9, 2115–2152, 2013

with a fully coupled ocean-atmosphere generalized circulation model (OAGCM), testing various East-Tethys seaway configurations. We particularly focus on the changes that occur in the Indian, Atlantic and Southern oceans, in order to explore the link between East-Tethys seaway, TISW formation and global oceanic circulation and climate.

2 Model and experiment design

FOAM (Fast Ocean Atmosphere Model) version 1.5 is a fully coupled OAGCM (Tobis et al., 1997). The atmospheric component is a parallelized version of Community Climate Model 2 (CCM2) developed at the National Center for Atmospheric Research (NCAR), with atmospheric physics upgraded following CCM3 (Tobis et al., 1997). The atmospheric component runs at R15 spatial resolution ($4.5^{\circ} \times 7.5^{\circ}$), with 18 vertical layers. The oceanic component is a parallel ocean model dynamically similar to the Geophysical Fluid Dynamics Laboratory's Modular Ocean Model (MOM) (Tobis et al., 1997). The spatial resolution of the oceanic component is a 128×128 Mercator grid ($1.4^{\circ} \times 2.8^{\circ}$), with 24 vertical levels. The atmospheric and oceanic components are linked by a coupler, which calculates and interpolates fluxes between the two components (Tobis et al., 1997). FOAMv1.5 compares well with other generalized circulation models for present-day climate (Jacob, 1997) and has also proven to be useful in the study of past climates (Poulsen et al., 2001; Donnadieu et al., 2006; Zhang et al., 2011; Chaboureau et al., 2012; Hamon et al., 2012; Lefebvre et al., 2012).

Our middle Miocene simulations are forced with a palaeogeography derived from Herold et al. (2008). The main differences compared to the present day geography are lower reliefs, an open Central American Isthmus, a closed Bering Strait and a southward shift of Australia (Fig. 1). This geography also includes a reduced ice sheet over Antarctica (Herold et al., 2008). Because the East-Tethys closure occurred progressively, it is interesting to explore ocean and climate response to different gateway configurations. We therefore performed four sensitivity experiments with various gateway depths (Table 1). The Miocene vegetation is based on Wolfe (1985) and is the same as

CPD
9, 2115–2152, 2013

used in previous studies on middle Miocene climate (Tong et al., 2009; You et al., 2009; Herold et al., 2009; Hamon et al., 2012). Important changes compared to present-day vegetation is the absence of desert, the larger latitudinal expansion of tropical and subtropical forests as well as the replacement of ice by boreal forest in Greenland.

As stated earlier, the atmospheric CO_2 concentration during the middle Miocene is still highly debated (Cerling, 1991; Pagani et al., 1999, 2009; Pearson and Palmer, 2000; Royer et al., 2001; Kürschner et al., 2008; Kürschner and Kvacek, 2009; Tripati et al., 2009). Recent modelling studies concluded that higher than present pCO_2 is necessary to simulate a middle Miocene climate consistent with data (Tong et al., 2009; You et al., 2009; Henrot et al., 2010; Krapp and Jungclaus, 2011; Hamon et al., 2012). Moreover, using the model FOAMv1.5, Hamon et al. (2012) showed that Miocene European climate and vegetation are more consistent with data when the pCO_2 is equal to 560 ppmv. In our four middle Miocene simulations, we therefore used this concentration. Solar constant, orbital parameters, pCH_4 and pN_2O were kept at their modern values. All the experiments were integrated for 1400 yr without flux correction. We use the average of the last 30 yr of each simulation for our analyses.

3 Results

3.1 Paratethys-Indian exchange and TISW formation

Over the Paratethys, the combination of high evaporation rates, low precipitation and low runoff from the adjacent continents leads to surface salinities scaling up to 37.5 psu (Fig. 2). The three experiments with an open East-Tethys depict a northward surface inflow entering the East-Tethys gateway. This inflow is linked to wind stress induced by boreal summer Indian monsoon winds that blow off the northeastern African coast (Fig. 3). In deep-open experiments (Mio4000 and Mio1000), this northward flow is restricted to the first 500 m, while below this depth a strong counter-current, driven by salinity gradient between the saline Paratethys and relative fresher Indian Ocean,

CPD
9, 2115–2152, 2013

brings water masses southward (Figs. 4c and 5). This result is consistent with a previous modelling study showing no northward water flux in the East-Tethys below 500 m (Fig. 11 in Butzin et al., 2011). However, most modelling studies (e.g. von der Heydt and Dijkstra, 2005; Herold et al., 2012) depict an overall net flow in the East-Tethys that is oriented towards the Paratethys with water transported from the Indian Ocean to the Atlantic through the Paratethys. In our simulations, the reversed flow ranges between 5.5 Sv (Mio4000) and 7.4 Sv (Mio1000), leading to an overall net southward outflow of 1.5–2 Sv (Fig. 4c and Table 2). This flow reversal in the East-Tethys seaway in the Mio4000 and Mio1000 experiments is due to the eastward water transport in the Gibraltar Strait (Fig. 4a), that do not allow the transport of water from the Indian Ocean towards the Atlantic. This is explained by (i) the difference of bathymetry between the East-Tethys (respectively 4000 and 1000 m) and the Gibraltar Strait (400 m) and (ii) the inflow of surface water coming from the subtropical Atlantic gyre to the Gibraltar Strait that induces eastward transport (Fig. 2). The outflow from the East-Tethys gateway induces the onset of warm and salty (up to 37.7 psu at 1000 m depth) waters in the Indian Ocean (Figs. 5 and 6), which is consistent with the TISW described on the basis of isotopic data (Woodruff and Savin, 1989; Wright et al., 1992; Flower and Kennett, 1994; Flower and Kennett, 1995).

Conversely, the shallow bathymetry of the Mio250 experiment allows only a weak subsurface northward current to flow in the East-Tethys gateway and prevents any southward countercurrent to develop, thereby precluding the formation of TISW (Figs. 4c, 5 and 6). As a consequence, compared to the two deep-open experiments Mio4000 and Mio1000, Mio250 depicts a cooling and freshening of the Indian Ocean that spreads down to 3000 m and to 60° S (Fig. 7), whereas the Paratethys displays higher salinity.

Mio250 and MioC experiments exhibit very similar patterns of temperature and salinity in the Indian Ocean, suggesting that only a deep East-Tethys seaway can produce the TISW (Fig. 6). However, the two simulations differ regarding the Paratethys salinity: Mio250 surface flow from the Indian Ocean to the Gibraltar Strait produces

CPD
9, 2115–2152, 2013

surface salinities that are 1 psu lower than the values simulated with a semi-enclosed Paratethys (experiment MioC).

3.2 Paratethys-Atlantic exchange and AMOC

In Mio4000 and Mio1000, the entire water flux through the Gibraltar Strait flows from the Atlantic to the Paratethys (Figs. 2, 4a and 5). When the East-Tethys is shoaled to 250 m, this flow is opposite to the inflow from the East-Tethys seaway, producing a net outflow to the Atlantic of approximately 2.8 Sv (Table 2). With this outflow, Atlantic Intermediate Water, between 750 and 2000 m, are warmer and saltier than in deep-open East-Tethys experiments (Fig. 7). When the East-Tethys is fully closed, Paratethys-Atlantic exchange is rather similar to modern Mediterranean-Atlantic exchange, with a surface eastward flow of North Atlantic Water in the Paratethys and a deeper (between 200 and 400 m) westward flow into the Atlantic (Figs. 4a and 5). The latter outflow feed the North Atlantic in a similar way than in Mio250 experiment, but the temperature and salinity anomalies compared to Mio4000 experiment do not reach the western boundary of the Atlantic basin. However, in both Mio250 and MioC, the southern part of the Atlantic Meridional Overturning Circulation (AMOC), indicated by the meridional streamfunction, is enhanced compared to Mio4000 (Fig. 8). This result is consistent with a recent study suggesting that the input of warm and saline water from the Mediterranean Sea strengthens the AMOC (Ivanovic et al., 2013).

3.3 Southern Ocean

The presence or absence of TISW in the Indian Ocean influences the latitudinal patterns of density. Figure 10a shows the vertical profile of the potential density anomaly between a southern box and a northern box in the Indian Ocean. It indicates that the absence of TISW in experiments Mio250 and MioC induces a stronger latitudinal density gradient. In turn, this gradient produces stronger meridional advection (not shown) and enhanced geostrophic westerly volume transport between depths of 200 and 2800 m

CPD
9, 2115–2152, 2013

(Fig. 9), which corresponds to a strengthening of the Antarctic Circumpolar Current (ACC). Moreover, the intensification of the AMOC due to the closure of the East-Tethys seaway may increase the pressure gradient in the Atlantic Ocean and reinforce the ACC. The shoaling to 250 m and the full closure of the East-Teathys seaway increase the total ACC volume transport in the Tasmanian gateway by 4.1 and 8.8 Sv respectively (i.e. 6.4 and 13.9 % respectively) when compared to Mio4000 (Table 2). As a consequence sea-surface temperatures are lower and sea-ice extent is increased, which produces denser water at southern high latitudes, therefore enhancing the latitudinal density gradient. Moreover, these colder surface temperatures affect the atmosphere and make the latitudinal thermal gradient stronger, ultimately reinforcing the westerlies strength, a positive feedback for the ACC.

3.4 Antarctic climate

The reorganisation of oceanic circulation due to the shoaling and closure of the East-Tethys seaway provokes surface temperature variations, especially over Antarctica. The decrease of sea-surface temperatures in Southern Ocean, as well as the reinforcement of the ACC, induce an annual mean cooling of approximately 0.1 to 2.5 °C over Antarctica between the experiments Mio4000 and MioC (Fig. 11a). Moreover, the warmest month temperature is up to 1.3 °C colder when the East-Tethys seaway is closed, which should limit the ablation of the ice-sheet during summer (Fig. 11b). However, temperature variations are small, and only non significant precipitation variations occur over Antarctica between the experiments Mio4000 and MioC (lower than 100 mm yr^{-1}, not shown). Although consequences on Antartica ice sheet building remain to be tested with a dedicated ice sheet model, the weak changes of temperature and precipitation between Mio4000 and MioC simulated over Antarctica suggest that the East-Tethys closure unlikely drove the East-Antarctic Ice Sheet growth during the middle Miocene. Moreover, the global deepwater cooling between the experiments Mio4000 and MioC is −0.7 °C, whereas data-based reconstructions estimate that deep water cooled by approximately 3 °C during the MMCT (Billups and Schrag,

CPD
9, 2115–2152, 2013

2002). These results strongly suggest that the closure of the East-Tethys was not the only driver of the MMCT.

4 Discussion

4.1 Impact of East-Tethys seaway closure on Miocene ocean and climate

Three different hypotheses were proposed to explain the way the East-Tethys seaway closure allowed Antarctic Ice Sheet growth during the MMCT. First, the termination of the TISW production should have provoked a decrease in southward heat transport (Woodruff and Savin, 1989; Flower and Kennett, 1994; Flower and Kennett, 1995). The simulated cooling of the Indian Ocean as a response of the shutdown of Paratethys throughflow is consistent with this hypothesis. Secondly, the termination of TISW production should have induced the acceleration of the ACC (Flower and Kennett, 1995; Kuhnert et al., 2009; Verducci et al., 2009). Our simulations depict the full mechanism leading from the East-Tethys closure to the ACC acceleration, which is in good agreement with this data-derived hypothesis. Finally, it was proposed that the closure of the East-Tethys seaway enhanced the AMOC and meridional heat transport in the Atlantic Ocean, increasing evaportation in the Southern Ocean and therefore precipitation over Antarctica (Wright et al., 1992). Although our results are congruent with a reinforcement of the AMOC, simulated response to East-Tethys closure do not show significant changes in precipitation over Antarctica.

Several modelling studies investigated the impact of geographic changes, and in particular seaways closure, on Cenozoic cooling (von der Heydt and Dijkstra, 2005, 2006; Zhang et al., 2011; Butzin et al., 2011). However two obstacles prevent a reliable intercomparison: the variety of models used, and the palaeogeography and experiment design involved. In this section we discuss some characteristics of previous studies to emphasize the need for an intercomparison project on the modeling of the impact of ocean gateways on climate. von der Heydt and Dijkstra (2005, 2006) focused on

CPD
9, 2115–2152, 2013

the impact of closing the East-Tethys seaway on Caribbean oceanic circulation and temperatures. Using CCSM1.4, with a very deep (5000 m) and wide Paratethys, they suggested that the closure of the East-Tethys and the opening of the Drake Passage induced a reversal of water transport in the Panama Seaway, provoking a local cooling in this region. Their experiments also depict an overestimated ACC, relatively low (ca. 4 Sv) eastward water transport in the Panama Seaway and a net westward (ca. 12 Sv) water flow in the East-Tethys. These results are consistent with an open Tethys experiment carried on with a later version of the model – CCSM3 – (Herold et al., 2012) but differ from ours, which depict a weak eastward Tethys throughflow and a strong eastward transport through Panama (not shown). The diverging responses with von der Heydt and Dijkstra (2005) study can be explained by important palaeogeography differences (they used idealized flat-bottom ocean (5000 m) and two geographic configurations corresponding to the late Oligocene and the early Miocene). However, our palaeogeography being the same as used in Herold et al. (2012), differences with the latter are more likely linked to model parameterizations and ocean-atmosphere coupling.

Zhang et al. (2011) used the model FOAM (same version as us) and showed that the East-Tethys and Panama seaways closure are key in the development of a modern-like oceanic circulation, dominated by North Atlantic deep water. Despite their early Eocene geographic configuration, their results show that a constriction of tropical gateways, including the East-Tethys, drives a drop of sea surface temperatures and surface salinity in the Indian Ocean. Using an ocean circulation carbon cycle model of intermediate complexity, Butzin et al. (2011) tested the impact of various seaways configurations on ocean circulation during the Miocene. Comparable with our study, water fluxes through the East-Tethys seaway are northward in surface, and southward at depth. By suppressing this southward water transport, the closure of the East-Tethys leads to a cooling of up to 4 °C between 500 and 2000 m, a result consistent with ours and with data (Zachos et al., 2001; Billups and Schrag, 2002). However, according to Butzin et al. (2011), this pattern strongly depends on the width of the East-Tethys seaway;

CPD
9, 2115–2152, 2013

a narrow East-Tethys produces an equilibrated throughflow (i.e. net flow approximately 0 Sv), whereas a wide East-Tethys leads to a surface northern flow that overcomes the deeper southern flow. Consequently, Butzin et al. (2011) find no large scale impact of the East-Tethys, especially on the ACC.

Our results highlight an intensification of the ACC when the East-Tethys seaway is closed compared as when it is open (Table 2), which is consistent with data-based reconstructions of oceanic circulation changes during the MMCT (Shevenell et al., 2004; Kuhnert et al., 2009). This discrepancy between model results can be due either to the difference in the boundary conditions (Butzin et al., 2011 used present-day geography with modified seaways and the ocean model they use is forced by present-day wind fields) or to the models themselves. New simulations and model intercomparisons should help us to understand the cause of this discrepancy between our results and those of Butzin et al. (2011), and therefore discuss the impact of the East-Tethys seaway closure on the circum-Antarctic circulation during the middle Miocene.

The temperature changes in the Indian Ocean between the MioC and Mio4000 experiments, in particular the strong cooling of deep water, is congruent with the results of Butzin et al. (2011) and with data (Zachos et al., 2001; Billups and Schrag, 2002). However, the heat transport variations due to the closure of the East-Tethys seaway cannot provide a satisfying explanation for the rapid growth of East Antarctica ice sheet, and the global cooling simulated between the Miocene experiments is too weak compared to the cooling deduced from data (Zachos et al., 2001; Billups and Schrag, 2002). Therefore the closure of the East-Tethys seaway was probably not the main cause of the MMCT, and other mechanisms should be tested to better understand this climatic transition.

4.2 Timing of the East-Tethys seaway closure

The timing of the East-Tethys seaway closure is not well constrained, paleontological, isotopic and geological evidences providing conflicting estimations (Rögl, 1999; Harzhauser and Piller, 2007; Harzhauser et al., 2009; Allen and Armstrong, 2008;

CPD
9, 2115–2152, 2013

Hüsing et al., 2009; Reuter et al., 2009; Okay et al., 2010). Some authors suggest a Late Eocene age (approximately 35 Ma) based on the study of deformation and uplift during the collision between the Afro-Arabian and Eurasian plates (Allen and Armstrong, 2008). Using apatite fission tracks datation and regional stratigraphy in the Zagros Basin, Okay et al. (2010) deduce that the collision between Afro-Arabia and Eurasia occurred in the early Miocene (approximately 20 Ma), which is consistent with the first evidence of mammal exchanges between the two continents (Rögl, 1999; Harzhauser and Piller, 2007). However, stratigraphic and oceanic paleontological data indicate that the Paratethys and the Indian Ocean basins were intermittently connected until at least the middle Miocene (Rögl, 1999; Harzhauser and Piller, 2007; Harzhauser et al., 2009; Okay et al., 2010; de Leeuw et al., 2013). The consensual view is that, after the initial collision between Afro-Arabia and Eurasia, the remaining East-Tethys seaway was not floored by oceanic crust, and the reopening phases were mainly due to sea-level changes (Rögl, 1999; Harzhauser and Piller, 2007; Harzhauser et al., 2009; Allen and Armstrong, 2008; Hüsing et al., 2009; Reuter et al., 2009; Okay et al., 2010). Therefore, a deep East-Tethys seaway, corresponding to the experiment Mio4000, is not consistent with data for the middle Miocene.

Many authors agree that the final closure of the East-Tethys seaway, and the subsequent end of water exchanges between the Paratethys and the Indian ocean, occurred during the middle Miocene, at approximately 14 Ma (Rögl, 1999; Harzhauser and Piller, 2007; Harzhauser et al., 2009; de Leeuw et al., 2013). This age estimation coincides with the middle Miocene climatic transition, and is one of the arguments supporting the hypothesis of the East-Tethys closure as a driver of this transition (Woodruff and Savin, 1989; Wright et al., 1992; Flower and Kennett, 1994; Flower and Kennett, 1995). However, recently Hüsing et al. (2009) suggested that the East-Tethys seaway final closure occurred at approximately 11 Ma, which is much younger than the previous estimations. Their work is based on the study of the evolution of foreland basins located in southern Turkey (Hüsing et al., 2009). They particularly suggested that deep marine conditions prevailed in this region during the early Tortonian (appoximately 11 Ma), providing

CPD
9, 2115–2152, 2013

a gateway between Mediterranean and Indian Ocean along the northern margin of Arabia (Hüsing et al., 2009).

Stable isotope composition of marine carbonates indicates the existence of TISW in the Indian Ocean during the early and middle Miocene (Woodruff and Savin, 1989; Wright et al., 1992; Flower and Kennett, 1994; Flower and Kennett, 1995). In the present study, we show that TISW cannot be produced when the East-Tethys seaway is shallow (250 m depth), water transport being from the Indian Ocean towards the Paratethys in the Mio250 experiment. Therefore we can assume that, prior to approximately 14 Ma, a relatively deep seaway (more than 250 m depth) connected the Indian Ocean and the Paratethys, allowing the production of TISW. Moreover, the termination of TISW production during the MMCT (Woodruff and Savin, 1989; Wright et al., 1992; Flower and Kennett, 1994; Flower and Kennett, 1995) suggests a middle Miocene age for the final closure of the East-Tethys seaway, which is consistent with oceanic paleontological data (Rögl, 1999; Harzhauser and Piller, 2007; Harzhauser et al., 2009; Reuter et al., 2009), but not with the study of Hüsing et al. (2009), who suggested that a connection between the Mediterranean Sea and the Indian Ocean still existed at 11 Ma.

The present study allows a better understanding of the impact of shallowing and closing the East-Tethys seaway, which can provide new constraints on the timing of this event. In particular, our results highlight the existence of TISW in the deep-open experiments, and the absence of this water mass in the Mio250 and MioC experiments. Isotopic data indicate that the termination of TISW formation occurred at approximately 14 Ma, that is during the MMCT. Therefore we can assume that, prior to 14 Ma, the East-Tethys seaway was deeper than 250 m, whereas it was shallower during the MMCT.

4.3 The cause of the middle Miocene climatic transition

Our results suggest that the East-Tethys seaway closure was crucial for ocean dynamics changes but was not the major cause of the MMCT. The reinforcement of the ACC

CPD
9, 2115–2152, 2013

due to the East-Tethys seaway closure probably amplified the cooling initiated by an other factor, for example an atmospheric CO_2 decrease or orbital parameter variations. Recent modelling studies have shown that high pCO_2 are necessary to simulate a climate and vegetation congruent with data during the middle Miocene climatic optimum (You et al., 2009; Tong et al., 2009; Henrot et al., 2010; Hamon et al., 2012). This is in agreement with terrestrial pCO_2 reconstructions (Royer et al., 2001; Kürschner et al., 2008; Kürschner and Kvacek, 2009), according to which an important atmospheric CO_2 concentration decrease (from ca. 500 to ca. 280 ppmv) occurred at 14 Ma.

Interestingly, Allen and Armstrong (2008) argued that the closure of the East-Tethys seaway played an important role in the early Oligocene glaciations in Antarctica. They particularly suggest that this tectonic event strongly impacted the carbon cycle, particularly through the oceanic circulation reorganisation (Allen and Armstrong, 2008). Although their estimation of the East-Tethys seaway closure predates the MMCT from approximately 20 Ma, the mechanisms they proposed to explain the pCO_2 drowdawn can provide a valuable explanation of the MMCT. In particular, they suggest that the closure of the East-Tethys provoked intensive storage of carbon in the Paratethys basins, and that the oceanic reorganisation induced an increase in organic productivity, therefore decreasing atmospheric CO_2 concentration (Allen and Armstrong, 2008). In our shallow and closed East-Tethys experiments, we observe an increase of Paratethys stratification compared to deep-open experiments (see Fig. 5), which could have favour carbon storage in this basin. In the same time, the elevation of the high reliefs, such as the Andes, the Alps, the Himalayas and the Tibetan Plateau, should have enhanced silicate weathering, contributing to the pCO_2 drowdawn during the middle Miocene (Gregory-Wodzicki, 2000; Foeken et al., 2003; Currie et al., 2005; Garzione et al., 2006, 2008). Future studies should combine climate and carbon cycle modeling with $\delta^{13}C$ analyses to test this hypothesis, and confirm or infirm the impact of East-Tethys closure on the global carbon cycle.

Recent modelling studies have investigated the impact of vaying pCO_2 on middle Miocene climate (Tong et al., 2009; You et al., 2009; Henrot et al., 2010; Krapp and

CPD
9, 2115–2152, 2013

Jungclaus, 2011; Hamon et al., 2012). In particular, Tong et al. (2009) demonstrated that doubling atmospheric CO_2 concentration in an atmospheric model forced with middle Miocene geography and vegetation induces a mean global warming between 2.1 and 2.4 °C. This sensitivity to doubled pCO_2 is higher in coupled ocean-atmosphere models (4.2 °C according to Krapp and Jungclaus, 2011 and 4.8 °C in Hamon et al., 2012).

For the present-day geographic configuration, the fourth IPCC report indicates a sensitivity to doubled pCO_2 between 2 and 4.5 °C, with a most probable value close to 3 °C. This suggests that the sensitivity to atmospheric pCO_2 was higher during the Miocene, which is due to the important changes in the oceanic circulation compared to present-day (Krapp and Jungclaus, 2011; Hamon et al., 2012). The closure of the East-Tethys seaway, by modifying the oceanic circulation, should therefore have an impact on climatic sensitivity to CO_2 concentration. New simulations testing varying atmospheric CO_2 concentrations with open and closed East-Tethys are therefore needed to better constrain the impact of pCO_2 on middle Miocene climate.

In summary, an important atmospheric pCO_2 decrease, possibly linked to the enhanced organic productivity and carbon storage in the Paratethys basins when the East-Tethys seaway closed, can be considered as an appropriate scenario of the East-Antarctic Ice Sheet growth and global cooling during the middle Miocene. This is consistent with the results of Deconto et al. (2007) and with terrestrial paleo-pCO_2 reconstructions (Royer et al., 2001; Kürschner et al., 2008; Kürschner and Kvacek, 2009). Moreover, the oceanic circulation reorganisation due to the closure of the East-Tethys seaway contributed to the thermic isolation of Antarctica, allowing the ice-sheet development. New simulations with various OAGCM should be useful to assess the respective roles of pCO_2, East-Tethys seaway closure and orbital configuration in the MMCT.

CPD
9, 2115–2152, 2013

5 Conclusions

In this work we investigated the impact of varying East-Tethys seaway configurations on middle Miocene oceanic circulation and climate. We performed four sensitivity experiments with various East-Tethys depths (4000, 1000, 250 and 0 m). We highlighted the existence of warm and saline deep water in the Indian Ocean when the East-Tethys seaway is deep-open (4000 or 1000 m), which corresponds to the TISW described in studies based on isotopic composition of benthic foraminifera (Woodruff and Savin, 1989; Wright et al., 1992; Flower and Kennett, 1994; Flower and Kennett, 1995). We demonstrated that the shoaling of the East-Tethys seaway to 250 m and ultimately its closure provoked the termination of TISW production, inducing important temperature and salinity changes in the Indian Ocean. This led to changes in the latitudinal density gradient and to the acceleration of the ACC. Moreover, when the East-Tethys seaway is closed or shallow, the warm and salty water from the Paratethys is transported in the Atlantic Ocean through the Gibraltar Strait, enhancing the AMOC. These results are in good agreement with isotopic studies (Woodruff and Savin, 1989; Wright et al., 1992; Flower and Kennett, 1994; Flower and Kennett, 1995; Kuhnert et al., 2009; Verducci et al., 2009), but differ from other modeling studies. New experiments with diverse ocean-atmosphere models, and consistent model intercomparison should be conducted in the future to better constrain the role of the East-Tethys seaway final closure in the middle Miocene oceanic circulation reorganisation.

Our results also bring new constraints on the East-Tethys seaway final closure. The presence of TISW in experiments with deep-open East-Tethys, and its absence in the shallow experiment, indicate that during the MMCT, when the TISW production terminated, the East-Tethys seaway was likely shallow. However, we cannot provide any information on the initial collision between Afro-Arabia and Eurasia, and further work is needed to bring new constraints on this event. More sensitivity experiments testing East-Tethys depth between 250 and 1000 m should also provide important constraints on the timing of the final closure of the East-Tethys seaway.

CPD
9, 2115–2152, 2013

The climatic changes caused by the East-Tethys seaway closure do not appear sufficient to explain the rapid ice-sheet growth over Antarctica during the MMCT. Another mechanism should have initiated the global cooling and the oceanic changes induced by the East-Tethys closure amplified its effects. Many authors have proposed a pCO_2 decrease as the main driver of the middle Miocene climatic transition and cryospheric expansion in Antarctica (Kürschner et al., 2008; Kürschner and Kvacek, 2009; Tripati et al., 2009). The recently published sensitivity tests on Miocene pCO_2 indicate that a drawdown of this gas concentration could have been key in the MMCT (Tong et al., 2009; You et al., 2009; Henrot et al., 2010; Krapp and Jungclaus, 2011; Hamon et al., 2012). However, new sensitivity experiments should be conducted to better understand the role of the atmospheric CO_2 concentration and of orbital configuration in the MMCT and the Antarctic ice-sheet growth.

Acknowledgements. We are particularly grateful to M. Brunet and the Collège de France, thanks to whom this work have been performed in the best circumstances. We also want to aknowledge Patrick Vignaud and the CNRS, as well as the CEA and Région Poitou-Charentes for the funding of this study. This work was performed using HPC resources from GENCI [CCRT/TGCC/CINES/IDRIS] (Grant 2013- [t2013012212]).

The publication of this article is financed by CNRS-INSU.

References

Allen, M. B. and Armstrong, H. A.: Arabia–Eurasia collision and the forcing of mid-Cenozoic global cooling, Palaeogeogr. Palaeocl., 265, 52–58, doi:10.1016/j.palaeo.2008.04.021, 2008. 2126, 2127, 2129

Billups, K. and Schrag, D.: Paleotemperatures and ice volume of the past 27 Myr revisited with paired Mg/Ca and $^{18}O/^{16}O$ measurements on benthic foraminifera, Paleoceanography, 17, 1003, doi:10.1029/2000PA000567, 2002. 2117, 2123, 2125, 2126

Bruch, A. A., Uhl, D., and Mosbrugger, V.: Miocene climate in Europepatterns and evolution: a first synthesis of NECLIME, Palaeogeogr. Palaeocl., 253, 1–7, doi:10.1016/j.palaeo.2007.03.030, 2007. 2117

Butzin, M., Lohmann, G., and Bickert, T.: Miocene ocean circulation inferred from marine carbon cycle modeling combined with benthic isotope records, Paleoceanography, 26, PA1203, doi:10.1029/2009PA001901, 2011. 2121, 2124, 2125, 2126

Cerling, T. E.: Carbon dioxide in the atmosphere: evidence from Cenozoic and Mesozoic paleosols, Am. J. Sci., 291, 377–400, doi:10.2475/ajs.291.4.377, 1991. 2117, 2120

Chaboureau, A.-C., Donnadieu, Y., Sepulchre, P., Robin, C., Guillocheau, F., and Rohais, S.: The Aptian evaporites of the South Atlantic: a climatic paradox?, Clim. Past, 8, 1047–1058, doi:10.5194/cp-8-1047-2012, 2012. 2119

Currie, B. S., Rowley, D. B., and Tabor, N. J.: Middle Miocene paleoaltimetry of southern Tibet: implications for the role of mantle thickening and delamination in the Himalayan orogen, Geology, 33, 181–184, doi:10.1130/G21170.1, 2005. 2129

Deconto, R. M., Pollard, D., and Harwood, D.: Sea ice feedback and Cenozoic evolution of Antarctic climate and ice sheets, Paleoceanography, 22, 1–18, doi:10.1029/2006PA001350, 2007. 2118, 2130

de Leeuw, A., Filipescu, S., Maţenco, L., Krijgsman, W., Kuiper, K., and Stoica, M.: Paleomagnetic and chronostratigraphic constraints on the Middle to Late Miocene evolution of the Transylvanian Basin (Romania): implications for Central Paratethys stratigraphy and emplacement of the Tisza-Dacia plate, Global Planet. Change, 2013, 82–98, doi:10.1016/j.gloplacha.2012.04.008, 2013. 2118, 2127

Donnadieu, Y., Pierrehumbert, R., Jacob, R., and Fluteau, F.: Modelling the primary control of paleogeography on Cretaceous climate, Earth Planet. Sc. Lett., 248, 426–437, doi:10.1016/j.epsl.2006.06.007, 2006. 2119

CPD
9, 2115–2152, 2013

Flower, B. P. and Kennett, J. P.: The middle Miocene climatic transition: East Antarctic Ice Sheet development, deep ocean circulation and global carbon cycling, Palaeogeogr. Palaeocl., 108, 537–555, doi:10.1016/0031-0182(94)90251-8, 1994. 2117, 2118, 2121, 2124, 2127, 2128, 2131

Flower, B. P. and Kennett, J. P.: Middle Miocene deepwater paleoceanography in the southwest Pacific: relations with East Antarctic Ice Sheet development, Paleoceanography, 10, 1095–1112, doi:10.1029/95PA02022, 1995. 2118, 2121, 2124, 2127, 2128, 2131

Foeken, J., Dunai, T., Bertotti, G., and Andriessen, P.: Late Miocene to present exhumation in the Ligurian Alps (southwest Alps) with evidence for accelerated denudation during the Messinian salinity crisis, Geology, 31, 797–800, doi:10.1130/G19572.1, 2003. 2129

Garzione, C. N., Molnar, P., Libarkin, J. C., and MacFadden, B. J.: Rapid late Miocene rise of the Bolivian Altiplano: evidence for removal of mantle lithosphere, Earth Planet. Sc. Lett., 241, 543–556, doi:10.1016/j.epsl.2005.11.026, 2006. 2129

Garzione, C. N., Hoke, G. D., Libarkin, J. C., Withers, S., MacFadden, B., Eiler, J., Ghosh, P., and Mulch, A.: Rise of the Andes, Science, 320, 1304–1307, doi:10.1126/science.1148615, 2008. 2129

Gregory-Wodzicki, K. M.: Uplift history of the Central and Northern Andes: a review, Geol. Soc. Am. Bull., 112, 1091–1105, doi:10.1130/0016-7606(2000)112<1091:UHOTCA>2.0.CO;2, 2000. 2129

Hamon, N., Sepulchre, P., Donnadieu, Y., Henrot, A.-J., François, L., Jaeger, J.-J., and Ramstein, G.: Growth of subtropical forests in Miocene Europe: the roles of carbon dioxide and Antarctic ice volume, Geology, 40, 567–570, doi:10.1130/G32990.1, 2012. 2119, 2120, 2129, 2130, 2132

Harzhauser, M. and Piller, W. E.: Benchmark data of a changing seapalaeogeography, palaeobiogeography and events in the Central Paratethys during the Miocene, Palaeogeogr. Palaeocl., 253, 8–31, doi:10.1016/j.palaeo.2007.03.031, 2007. 2118, 2126, 2127, 2128

Harzhauser, M., Reuter, M., Piller, W. E., Berning, B., Kroh, A., and Mandic, O.: Oligocene and Early Miocene gastropods from Kutch (NW India) document an early biogeographic switch from Western Tethys to Indo-Pacific, Palaeont. Z., 83, 333–372, doi:10.1007/s12542-009-0025-5, 2009. 2118, 2126, 2127, 2128

Henrot, A.-J., François, L., Favre, E., Butzin, M., Ouberdous, M., and Munhoven, G.: Effects of CO_2, continental distribution, topography and vegetation changes on the climate at the

CPD
9, 2115–2152, 2013

Middle Miocene: a model study, Clim. Past, 6, 675–694, doi:10.5194/cp-6-675-2010, 2010. 2120, 2129, 2132
Herold, N., Seton, M., Müller, R., You, Y., and Huber, M.: Middle Miocene tectonic boundary conditions for use in climate models, Geochem. Geophy. Geosy., 9, Q10009, doi:10.1029/2008GC002046, 2008. 2119
Herold, N., You, Y., Müller, R., and Seton, M.: Climate model sensitivity to changes in Miocene paleotopography, Aust. J. Earth Sci., 56, 1049–1059, doi:10.1080/08120090903246170, 2009. 2120
Herold, N., Huber, M., Müller, R., and Seton, M.: Modeling the Miocene climatic optimum: ocean circulation, Paleoceanography, 27, PA1209, doi:10.1029/2010PA002041, 2012. 2121, 2125
Holbourn, A., Kuhnt, W., Schulz, M., and Erlenkeuser, H.: Impacts of orbital forcing and atmospheric carbon dioxide on Miocene ice-sheet expansion, Nature, 438, 483–487, doi:10.1038/nature04123, 2005. 2117, 2118
Hüsing, S. K., Zachariasse, W.-J., van Hinsbergen, D. J., Krijgsman, W., Inceöz, M., Harzhauser, M., Mandic, O., and Kroh, A.: Oligocene–Miocene basin evolution in SE Anatolia, Turkey: constraints on the closure of the eastern Tethys gateway, Geological Society, London, Special Publications, 311, 107–132, doi:10.1144/SP311.4, 2009. 2127, 2128
Ivanovic, R. F., Valdes, P. J., Gregoire, L., Flecker, R., and Gutjahr, M.: Sensitivity of modern climate to the presence, strength and salinity of Mediterranean-Atlantic exchange in a global general circulation model, Clim. Dynam., doi:10.1007/s00382-013-1680-5, in press, 2013. 2122
Jacob, R. L.: Low frequency variability in a simulated atmosphere ocean system, Ph. D. thesis, University of Wisconsin, 1997. 2119
Krapp, M. and Jungclaus, J. H.: The Middle Miocene climate as modelled in an atmosphere-ocean-biosphere model, Clim. Past, 7, 1169–1188, doi:10.5194/cp-7-1169-2011, 2011. 2120, 2129, 2130, 2132
Kürschner, W. M. and Kvacek, Z.: Oligocene-Miocene CO_2 fluctuations, climatic and palaeofloristic trends inferred from fossil plant assemblages in central Europe, B. Geosci., 84, 189–202, doi:0.3140/bull.geosci.1091, 2009. 2117, 2120, 2129, 2130, 2132
Kürschner, W. M., Kvaček, Z., and Dilcher, D. L.: The impact of Miocene atmospheric carbon dioxide fluctuations on climate and the evolution of terrestrial ecosystems, P. Natl. Acad. Sci. USA, 105, 449–453, doi:10.1073/pnas.0708588105, 2008. 2117, 2120, 2129, 2130, 2132

CPD
9, 2115–2152, 2013

Kuhnert, H., Bickert, T., and Paulsen, H.: Southern Ocean frontal system changes precede Antarctic Ice Sheet growth during the middle Miocene, Earth Planet. Sc. Lett., 284, 630–638, doi:10.1016/j.epsl.2009.05.030, 2009. 2117, 2118, 2124, 2126, 2131

Lefebvre, V., Donnadieu, Y., Sepulchre, P., Swingedouw, D., and Zhang, Z.-S.: Deciphering the role of southern gateways and carbon dioxide on the onset of the Antarctic Circumpolar Current, Paleoceanography, 27, PA4201, doi:10.1029/2012PA002345, 2012. 2119

Mosbrugger, V., Utescher, T., and Dilcher, D. L.: Cenozoic continental climatic evolution of Central Europe, P. Natl. Acad. Sci. USA, 102, 14964–14969, doi:10.1073/pnas.0505267102, 2005. 2117

Okay, A. I., Zattin, M., and Cavazza, W.: Apatite fission-track data for the Miocene Arabia-Eurasia collision, Geology, 38, 35–38, doi:10.1130/G30234.1, 2010. 2118, 2127

Pagani, M., Arthur, M. A., and Freeman, K. H.: Miocene evolution of atmospheric carbon dioxide, Paleoceanography, 14, 273–292, doi:10.1029/1999PA900006, 1999. 2117, 2120

Pagani, M., Caldeira, K., Berner, R., and Beerling, D. J.: The role of terrestrial plants in limiting atmospheric CO_2 decline over the past 24 million years, Nature, 460, 85–88, doi:10.1038/nature08133, 2009. 2117, 2120

Pearson, P. N. and Palmer, M. R.: Atmospheric carbon dioxide concentrations over the past 60 million years, Nature, 406, 695–699, doi:10.1038/35021000, 2000. 2117, 2120

Poulsen, C. J., Pierrehumbert, R. T., and Jacob, R. L.: Impact of ocean dynamics on the simulation of the Neoproterozoic "snowball Earth", Geophys. Res. Lett., 28, 1575–1578, doi:10.1029/2000GL012058, 2001. 2119

Reuter, M., Piller, W., Harzhauser, M., Mandic, O., Berning, B., Rögl, F., Kroh, A., Aubry, M.-P., Wielandt-Schuster, U., and Hamedani, A.: The Oligo-/Miocene Qom Formation (Iran): evidence for an early Burdigalian restriction of the Tethyan Seaway and closure of its Iranian gateways, Int. J. Earth Sci., 98, 627–650, doi:10.1007/s00531-007-0269-9, 2009. 2127, 2128

Rögl, F.: Mediterranean and Paratethys. Facts and hypotheses of an Oligocene to Miocene paleogeography (short overview), Geol. Carpath., 50, 339–349, 1999. 2118, 2126, 2127, 2128

Royer, D. L., Wing, S. L., Beerling, D. J., Jolley, D. W., Koch, P. L., Hickey, L. J., and Berner, R. A.: Paleobotanical evidence for near present-day levels of atmospheric CO_2 during part of the Tertiary, Science, 292, 2310–2313, doi:10.1126/science.292.5525.2310, 2001. 2117, 2120, 2129, 2130

CPD
9, 2115–2152, 2013

Shevenell, A. E., Kennett, J. P., and Lea, D. W.: Middle Miocene southern ocean cooling and Antarctic cryosphere expansion, Science, 305, 1766–1770, doi:10.1126/science.1100061, 2004. 2117, 2118, 2126

Shevenell, A. E., Kennett, J. P., and Lea, D. W.: Middle Miocene Ice Sheet dynamics, deep-sea temperatures, and carbon cycling: a Southern Ocean perspective, Geochem. Geophy. Geosy., 9, Q02006, doi:10.1029/2007GC001736, 2008. 2117, 2118

Tobis, M., Schafer, C., Foster, I., Jacob, R., and Anderson, J.: FOAM: expanding the horizons of climate modeling, in: Supercomputing, ACM/IEEE 1997 Conference, San Jose, California, p. 27–27, doi:10.1145/509593.509620, 1997. 2119

Tong, J., You, Y., Müller, R., and Seton, M.: Climate model sensitivity to atmospheric CO_2 concentrations for the middle Miocene, Global Planet. Change, 67, 129–140, doi:10.1016/j.gloplacha.2009.02.001, 2009. 2120, 2129, 2130, 2132

Tripati, A. K., Roberts, C. D., and Eagle, R. A.: Coupling of CO_2 and ice sheet stability over major climate transitions of the last 20 million years, Science, 326, 1394–1397, doi:10.1126/science.1178296, 2009. 2117, 2120, 2132

Utescher, T., Bruch, A. A., Micheels, A., Mosbrugger, V., and Popova, S.: Cenozoic climate gradients in Eurasiaa palaeo-perspective on future climate change?, Palaeogeogr. Palaeocl., 304, 351–358, doi:10.1016/j.palaeo.2010.09.031, 2011. 2117

Verducci, M., Foresi, L., Scott, G., Sprovieri, M., Lirer, F., and Pelosi, N.: The Middle Miocene climatic transition in the Southern Ocean: evidence of paleoclimatic and hydrographic changes at Kerguelen plateau from planktonic foraminifers and stable isotopes, Palaeogeogr. Palaeocl., 280, 371–386, doi:10.1016/j.palaeo.2009.06.024, 2009. 2117, 2118, 2124, 2131

von der Heydt, A. and Dijkstra, H. A.: Flow reorganizations in the Panama Seaway: a cause for the demise of Miocene corals?, Geophys. Res. Lett., 32, L02609, doi:10.1029/2004GL020990, 2005. 2121, 2124, 2125

von der Heydt, A. and Dijkstra, H. A.: Effect of ocean gateways on the global ocean circulation in the late Oligocene and early Miocene, Paleoceanography, 21, PA1011, doi:10.1029/2005PA001149, 2006. 2124

Wolfe, J.: Distribution of major vegetational types during the Tertiary, in: The Carbon Cycle and Atmospheric CO_2: Natural Variations Archaean to Present, edited by: Sundquist, E. and Broecker, W., American Geophysical Union Monograph, Washington, DC, 32, 357–375, doi:10.1029/GM032p0357, 1985. 2119

CPD
9, 2115–2152, 2013

Woodruff, F. and Savin, S. M.: Miocene deepwater oceanography, Paleoceanography, 4, 87–140, doi:10.1029/PA004i001p00087, 1989. 2117, 2118, 2121, 2124, 2127, 2128, 2131

Wright, J. D., Miller, K. G., and Fairbanks, R. G.: Early and middle Miocene stable isotopes: implications for deepwater circulation and climate, Paleoceanography, 7, 357–389, doi:10.1029/92PA00760, 1992. 2118, 2121, 2124, 2127, 2128, 2131

You, Y., Huber, M., Müller, R., Poulsen, C., and Ribbe, J.: Simulation of the middle Miocene climate optimum, Geophys. Res. Lett., 36, L04702, doi:10.1029/2008GL036571, 2009. 2120, 2129, 2132

Zachos, J., Pagani, M., Sloan, L., Thomas, E., and Billups, K.: Trends, rhythms, and aberrations in global climate 65 Ma to present, Science, 292, 686–693, doi:10.1126/science.1059412, 2001. 2117, 2125, 2126

Zhang, Z., Nisancioglu, K. H., Flatøy, F., Bentsen, M., Bethke, I., and Wang, H.: Tropical seaways played a more important role than high latitude seaways in Cenozoic cooling, Clim. Past, 7, 801–813, doi:10.5194/cp-7-801-2011, 2011. 2119, 2124, 2125

CPD
9, 2115–2152, 2013

Table 1. East-Tethys seaway depth for each of the four sensitivity experiments.

Experiment	East-Tethys depth (m)
Mio4000	4000
Mio1000	1000
Mio250	250
MioC	0 (closed seaway)

CPD
9, 2115–2152, 2013

Table 2. Northward water transport (Sv) in the East-Tethys, and eastward water transport (Sv) in Gibraltar, Drake and Tasmanian seaways for each of the four Miocene experiments.

Experiment	East-Tethys	Gibraltar	Drake	Tasmanian
Mio4000	−1.7	2.6	43.0	62.8
Mio1000	−2.0	2.6	40.1	61.2
Mio250	2.7	−2.8	47.1	66.9
MioC	–	0	51.3	71.5

CPD
9, 2115–2152, 2013

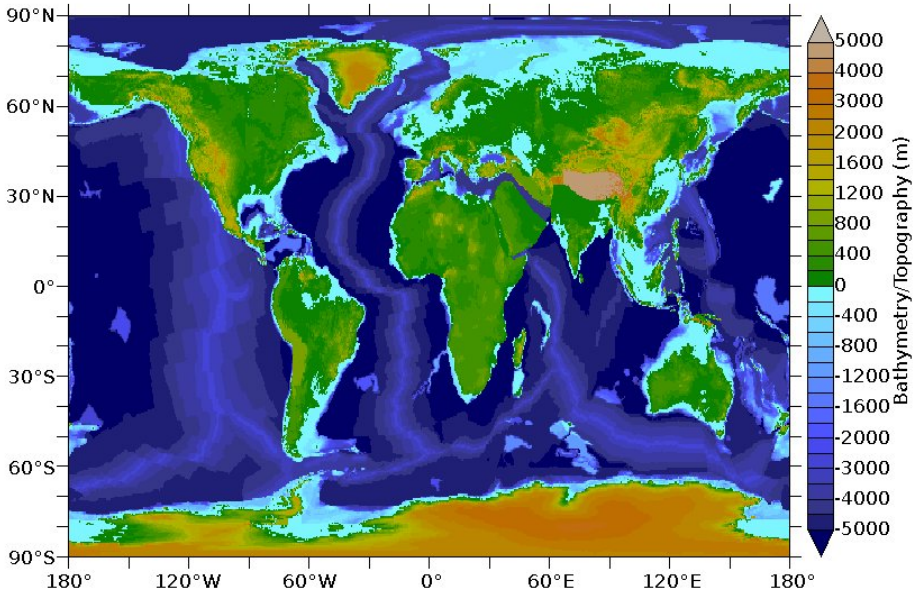

Fig. 1. Middle Miocene geography used in the Mio4000 experiment (East-Tethys seaway depth = 4000 m).

CPD
9, 2115–2152, 2013

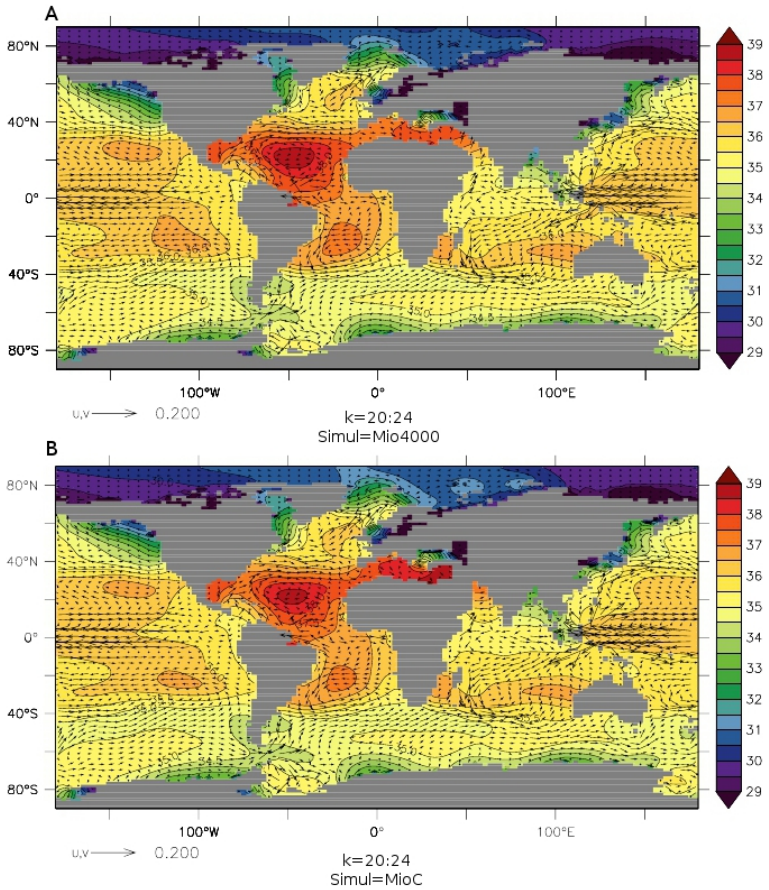

Fig. 2. Simulated annual salinity (psu) averaged over the top 100 m of the water column for Mio4000 **(A)** and MioC **(B)** experiments. Vectors indicate annual surface horizontal flow ($cm\,s^{-1}$).

CPD
9, 2115–2152, 2013

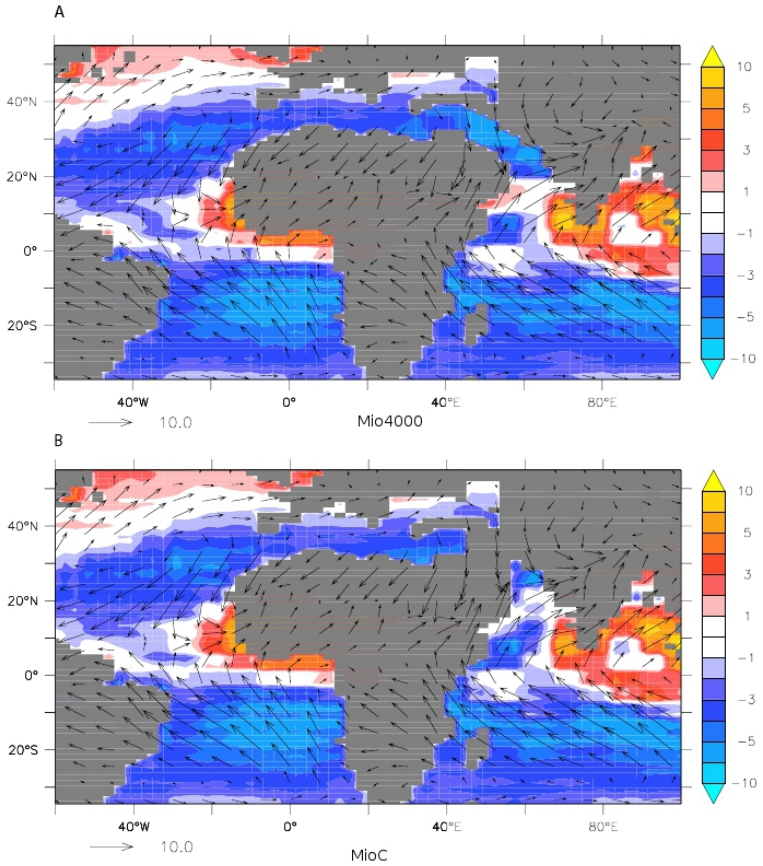

Fig. 3. Simulated boreal summer Precipitation minus Evaporation rate ($mm\,day^{-1}$) for Mio4000 **(A)** and MioC **(B)** experiments. Vectors indicate summer surface wind speed ($m\,s^{-1}$).

CPD
9, 2115–2152, 2013

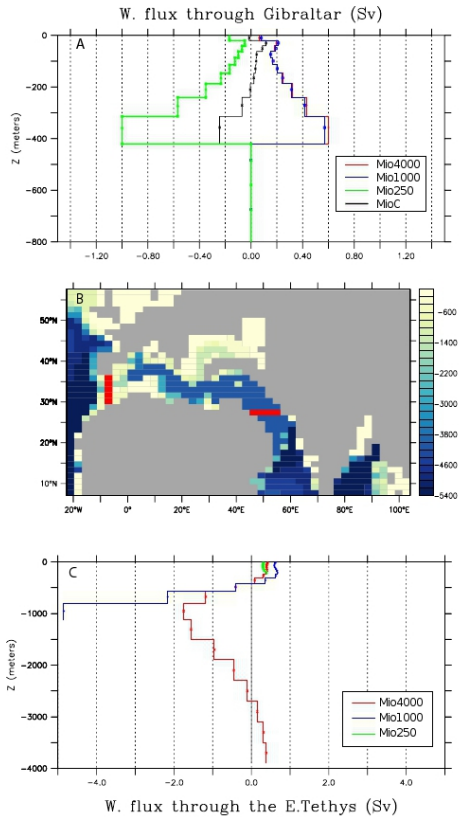

Fig. 4. (A) Zonal water transport through Gibraltar seaway (Sv). Positive values indicate eastward transport; negative values indicate westward transport. **(B)** Focus on bathymetry used in open East-Tethys experiments. Red segments indicate gridpoints where water transports have been computed. **(C)** Meridional water transport through East-Tethys seaway (Sv). Positive values indicate northward transport; negative values indicate southward transport.

CPD
9, 2115–2152, 2013

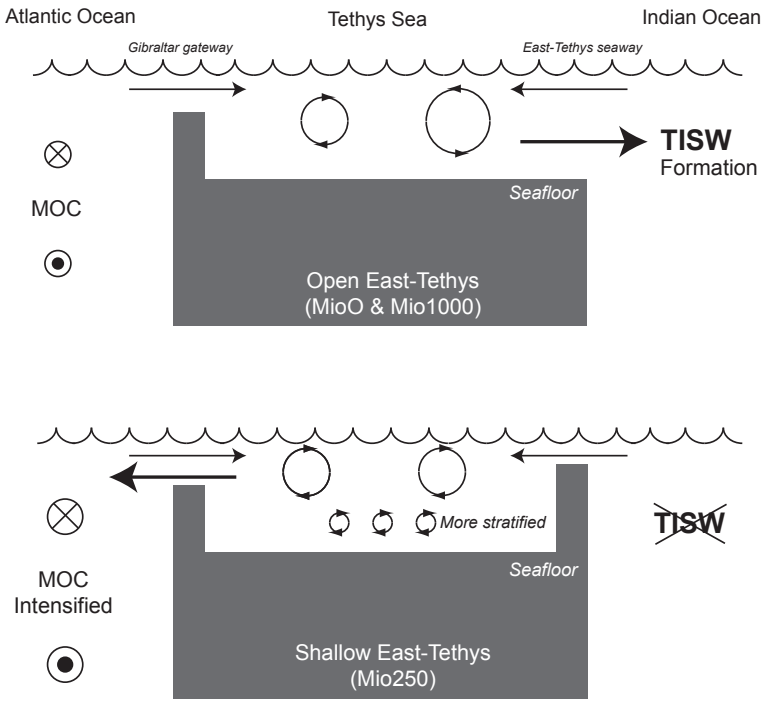

Fig. 5. Schematic view of oceanic circulation between the Indian Ocean, the Paratethys and the Atlantic Ocean when the East-Tethys seaway is deep-open (top panel) and when it is shallow (bottom panel).

CPD
9, 2115–2152, 2013

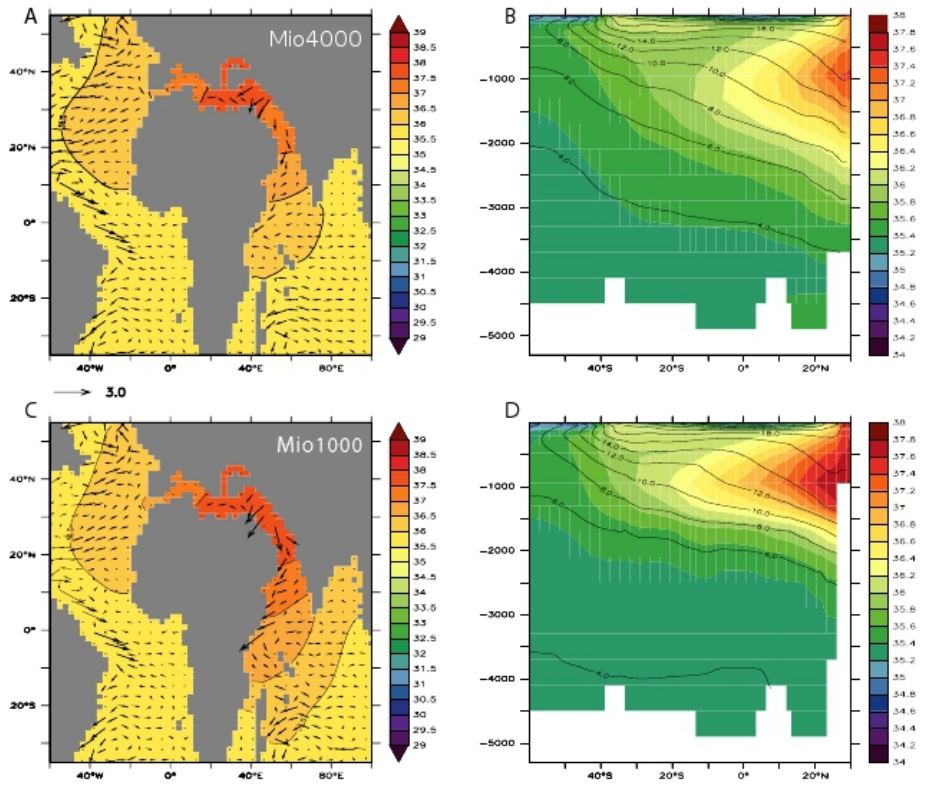

Fig. 6. Caption on next page.

CPD
9, 2115–2152, 2013

East-Tethys closure and middle Miocene climatic transition

N. Hamon et al.

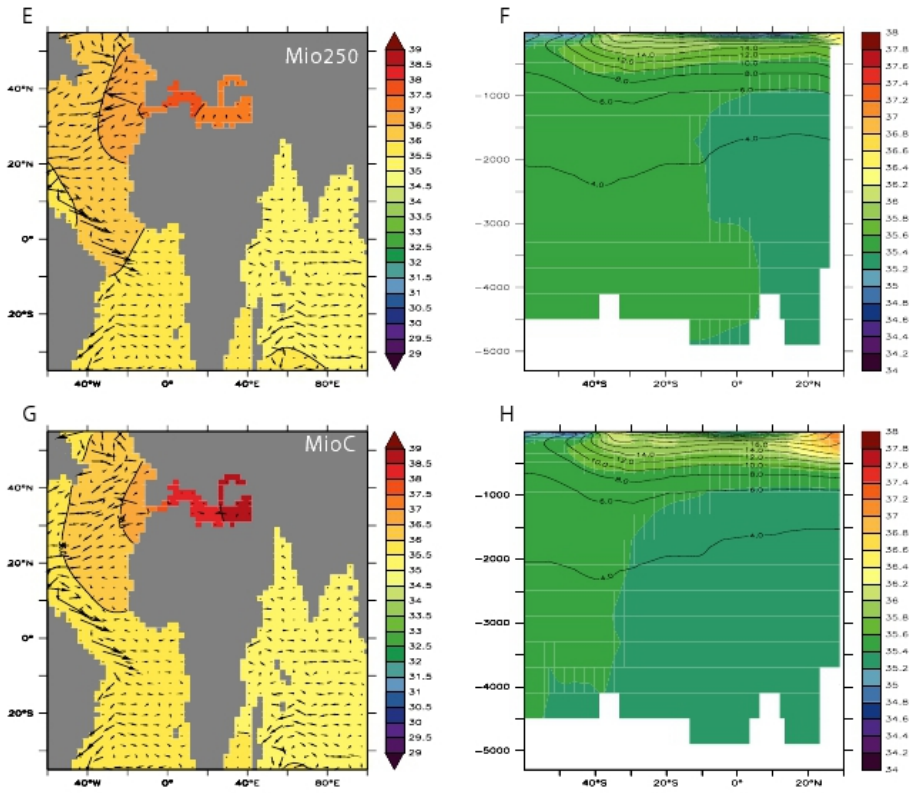

Fig. 6. (A, C, E, G) Simulated annual salinity at 952 m and horizontal flow (cm s^{-1}) for Mio4000, Mio1000, Mio250 and MioC, respectively. **(B, D, F, H)** Simulated salinity (shaded colors, psu) and temperature (isolines, °C) as a function of depth averaged between 45° E and 60° E, for Mio4000, Mio1000, Mio250 and MioC, respectively.

CPD
9, 2115–2152, 2013

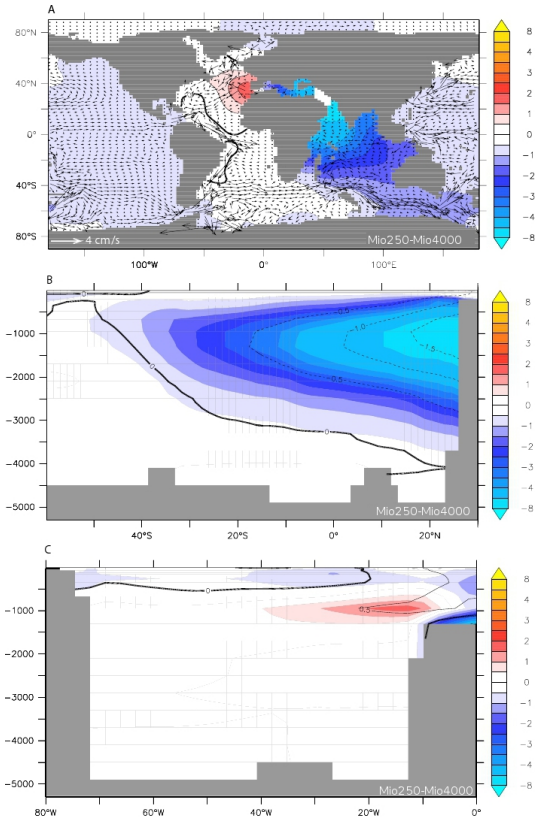

Fig. 7. (A) Simulated temperature difference at 952 m between Mio250 and Mio4000 experiments. Vectors indicate Mio4000 horizontal flow. **(B)** Mio250–Mio4000 anomaly of temperature (shaded colors, ˚C) and salinity (isolines, psu) as a function of depth, averaged between 45˚ E and 60˚ E. **(C)** Mio250–Mio4000 anomaly of temperature (shaded colors, ˚C) and salinity (isolines, psu) as a function of depth, averaged between 30˚ N and 40˚ N.

CPD
9, 2115–2152, 2013

East-Tethys closure and middle Miocene climatic transition

N. Hamon et al.

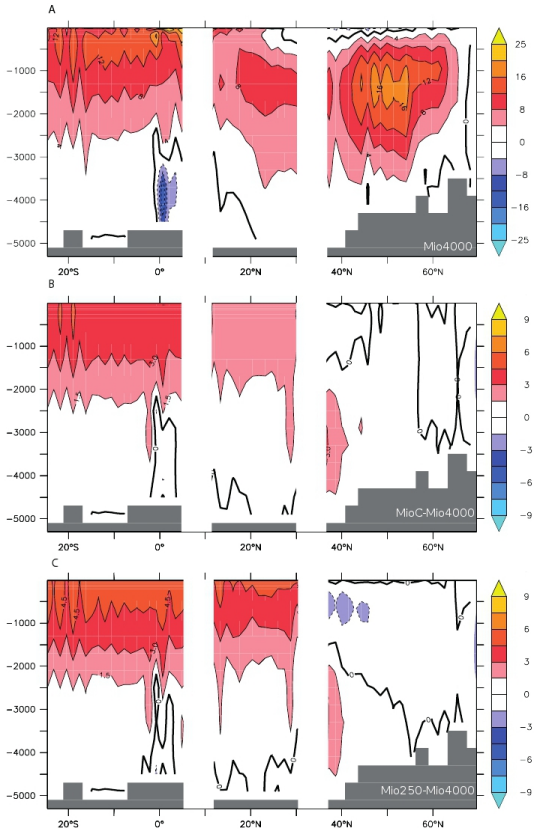

Fig. 8. (A) Simulated Atlantic meridional streamfunction for Mio4000 experiment. **(B)** MioC–Mio4000 Atlantic streamfunction anomaly. **(C)** Mio250–Mio4000 Atlantic streamfunction anomaly. Regions where divergence is not equal to zero have been masked.

CPD
9, 2115–2152, 2013

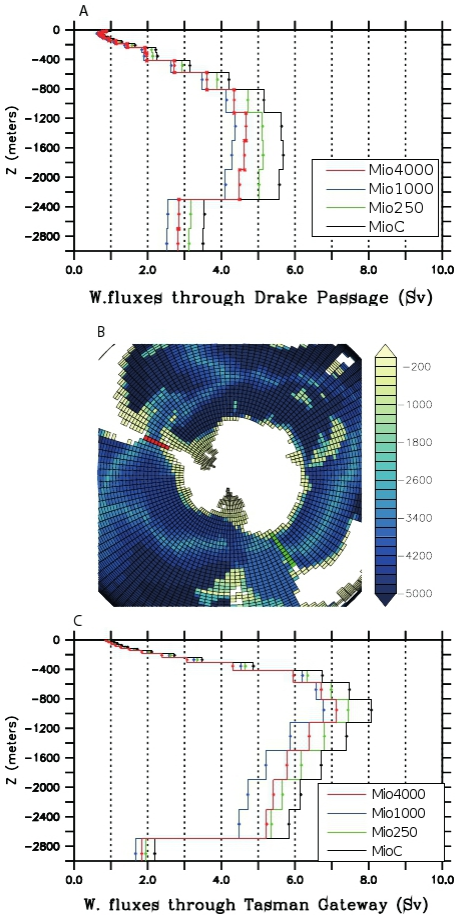

Fig. 9. (A, C) Zonal water transport through Drake **(A)** and Tasman **(C)** gateways, for the four experiments. **(B)** Focus on bathymetry used in all experiments. Colored segments indicate gridpoints where water transports have been computed.

CPD
9, 2115–2152, 2013

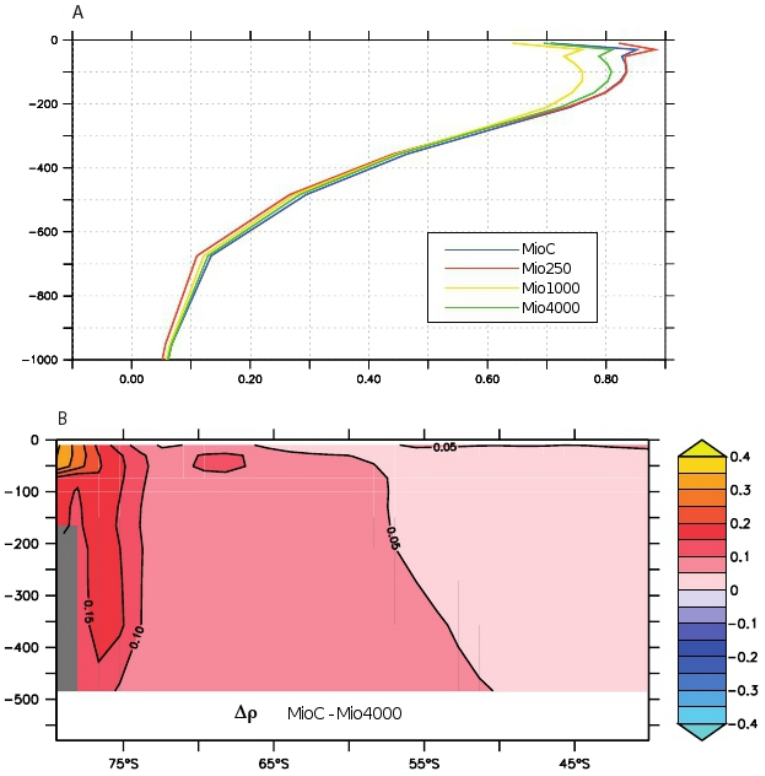

Fig. 10. (A) Simulated potential density ($kg\,m^{-3}$ – 1000) anomaly between a southern box (70° S–55° S) and a northern box (55° S–35° S) in the Indian Ocean (40° E–75° E), as a function of depth. **(B)** Simulated potential density anomaly ($kg\,m^{-3}$) between MioC and Mio4000 in the Indian Ocean.

CPD
9, 2115–2152, 2013

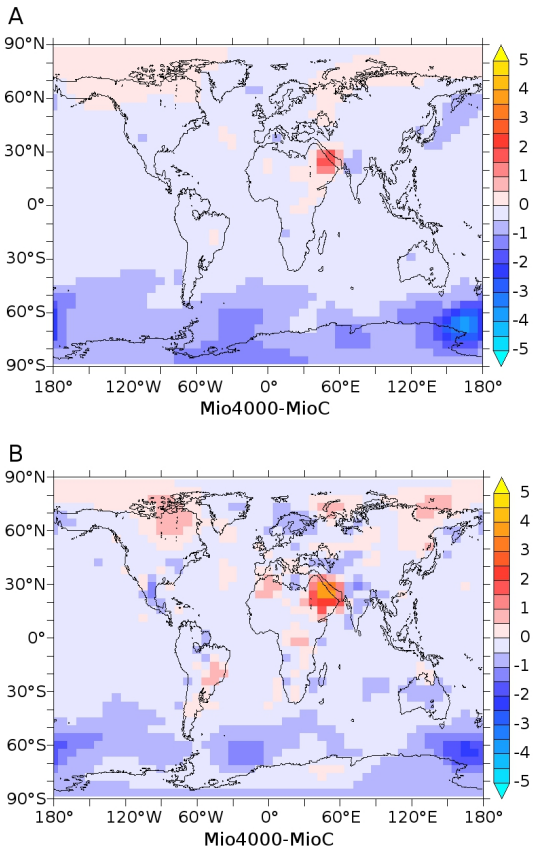

Fig. 11. Surface air temperature anomaly (˚C) between the experiments MioC and Mio4000. **(A)** Annual mean. **(B)** Warmest month.

CPD
9, 2115–2152, 2013